Nonlinear filter characteristics from an asynchronous cellular automaton oscillator

Hironori Ishimoto†, Masato Izawa‡, and Hiroyuki Torikai*

†Sharp Corporation, Yao, Osaka, Japan.
‡Graduate School of Engineering Science, Osaka University, Toyonaka, Osaka, Japan.
*Department of Computer Science, Kyoto Sangyo University, Kyoto, Japan.
Email: izawa@hopf.sys.es.osaka-u.ac.jp, torikai@cse.kyoto-su.ac.jp

Abstract—A coupled system of two asynchronous cellular automaton oscillators is introduced. It is shown that the coupled system can realize various nonlinear filter characteristics. Potential applications of the coupled system are also discussed.

1. Introduction

Recently, asynchronous cellular automaton neuron models have been investigated [1]-[6], the advantages and significances of which include the following points (see also [1] and references therein). (a) The asynchronous cellular automaton neuron model can be implemented by a reconfigurable hardware such as *field programmable gate array* (ab. FPGA). A control parameter of the model is a pattern of reconfigurable wires in a sequential logic circuit, and thus the parameter can be dynamically tuned by utilizing a dynamic reconfiguration function of the FPGA. Hence the asynchronous cellular automaton neuron model is suited for on-chip learning. On the other hand, dynamic parameter tuning of an analog circuit neuron model is often cumbersome. (b) The asynchronous cellular automaton neuron model consumes less hardware resources than the digital processor neuron for a wide range of reasonable parameter values. Also, unlike the digital processor neuron, the asynchronous cellular automaton neuron model uses no peripheral circuitry that plays no essential role to reproduce the nonlinear dynamics of a neuron. As a result, we can say that the asynchronous cellular automaton neuron model is a *compact and low-power hardware neuron model*. (c) Due to its compact and low-power features, the asynchronous cellular automaton neuron model is suited for many applications such as neural prosthesis chip and special hardware for large scale brain simulation. (d) From an academic viewpoint, modeling of the nonlinear dynamics of a biological system by a new way (e.g., modeling of the neuron's dynamics by the asynchronous cellular automaton like this paper) *per se* is an important research topic.

In this paper, a coupled system of two asynchronous cellular automaton oscillators is introduced [6]. It is shown that the coupled system can realize various nonlinear filter characteristics. Potential applications of the coupled system are also discussed.

2. Coupled system of two asynchronous cellular automaton oscillators

Let us refer to two asynchronous cellular automaton oscillators as O_I and O_O, where the indices I and O implicitly imply an *inner hair cell* and an *outer hair cell* in the mammalian cochlea but these implications are not very emphasized in this paper. The coupled system has the following discrete states.

Discrete states of O_I
$V_I \in \{0, 1, \cdots, M_I - 1\}$, $U_I \in \{0, 1, \cdots, N_I - 1\}$,

Discrete states of O_O
$V_O \in \{0, 1, \cdots, M_O - 1\}$, $U_O \in \{0, 1, \cdots, N_O - 1\}$,

Discrete state for coupling
$x \in \{0, 1, \cdots, L - 1\}$.

The oscillators O_I and O_O accept two independent clocks $C_I(t)$ and $C_O(t)$ with periods f_I and f_O, respectively. As preparation to construct vector fields of the oscillators O_I and O_O, the following functions are introduced.

Functions used to construct vector fields of O_I and O_O

$$n_{V_I}(V_I^*) = \alpha(\lfloor k_1 V_I^* + k_2 \rfloor, N_I),$$
$$n_{U_I}(V_I^*) = \alpha(\lfloor k_3 V_I^* + k_4 \rfloor, N_I),$$
$$n_{V_O}(V_O^*) = \alpha(\lfloor k_5 V_O^* + k_6 \rfloor, N_O),$$
$$n_{U_O}(V_O^*) = \alpha(\lfloor k_7 V_O^* + k_8 \rfloor, N_O),$$
$$\alpha(z, J) = \begin{cases} -1 & \text{if } z < -1, \\ z & \text{if } -1 \le z \le J, \\ J & \text{otherwise,} \end{cases}$$

where $\lfloor \cdot \rfloor$ is the floor function and

$$k_1 = \frac{n_1 N_I}{M_I},\ k_2 = \lfloor n_2 N_I \rfloor, k_3 = \frac{n_3 N_I}{M_I},\ k_4 = \lfloor n_4 N_I \rfloor,$$
$$k_5 = \frac{n_5 N_O}{M_O},\ k_6 = \lfloor n_6 N_O \rfloor, k_7 = \frac{n_7 N_O}{M_O},\ k_8 = \lfloor n_8 N_O \rfloor.$$

For simplicity, let us introduce the following notations.

"↑" denotes "*a positive edge of a clock.*"
":=" denotes "*an instantaneous transition of a discrete state.*"

Then the state transitions of the oscillators O_I and O_O induced by the clocks $C_I(t)$ and $C_O(t)$ are described by the

following equations, respectively.

State transitions of O_I induced by clock $C_I(t)$

If $C_I(t) = \uparrow$, then

$$V_I(t) := \begin{cases} V_S & \text{if } V_I = V_S, U_I < n_{V_I}(V_I^*), \\ M_I - 1 & \text{if } V_I = M_I - 1, U_I > n_{V_I}(V_I^*), \\ V_I - 1 & \text{if } V_I \neq V_S, U_I < n_{V_I}(V_I^*), \\ V_I + 1 & \text{if } V_I \neq M_I - 1, U_I > n_{V_I}(V_I^*), \\ V_I & \text{otherwise } (U_I = n_{V_I}(V_I^*)), \end{cases}$$

$$U_I(t) := \begin{cases} 0 & \text{if } U_I = 0, U_I > n_{U_I}(V_I^*), \\ N_I - 1 & \text{if } U_I = N_I - 1, U_I < n_{U_I}(V_I^*), \\ U_I - 1 & \text{if } U_I \neq 0, U_I > n_{U_I}(V_I^*), \\ U_I + 1 & \text{if } U_I \neq N_I - 1, U_I < n_{U_I}(V_I^*), \\ U_I & \text{otherwise } (U_I = n_{U_I}(V_I^*)). \end{cases}$$

State transitions of O_O induced by clock $C_O(t)$

If $C_O(t) = \uparrow$, then

$$V_O(t) := \begin{cases} 0 & \text{if } V_O = V_S, U_O < n_{V_O}(V_O^*), \\ M_O - 1 & \text{if } V_O = M_O - 1, U_O > n_{V_O}(V_O^*), \\ V_O - 1 & \text{if } V_O \neq 0, U_O < n_{V_O}(V_O^*), \\ V_O + 1 & \text{if } V_O \neq M_O - 1, U_O > n_{V_O}(V_O^*), \\ V_O & \text{otherwise } (U_I = n_{V_O}(V_O^*)), \end{cases}$$

$$U_O(t) := \begin{cases} 0 & \text{if } U_O = 0, U_O > n_{U_O}(V_O^*), \\ N_O - 1 & \text{if } U_O = N_O - 1, U_O < n_{U_O}(V_O^*), \\ U_O - 1 & \text{if } U_O \neq 0, U_O > n_{U_O}(V_O^*), \\ U_O + 1 & \text{if } U_O \neq N_O - 1, U_O < n_{U_O}(V_O^*), \\ U_O & \text{otherwise } (U_O = n_{U_O}(V_O^*)). \end{cases}$$

Also, let us introduce the following saturation set

Saturation set

$$\mathbf{V_S} = \{(V_I, U_I) \mid V_I = V_S\}$$

on which the state vector (V_I, U_I) is saturated. In addition to the clocks $C_I(t)$ and $C_O(t)$, the oscillators O_I and O_O accept a stimulation spike-train $S(t)$. The state transitions of the oscillators O_I and O_O induced by the stimulation spike-train $S(t)$ are described by the following equation.

State transitions induced by stimulation $S(t)$

If $S(t) = \uparrow$, then

$$V_I(t) := \begin{cases} V_S & \text{if } V_O = V_S, \\ V_I - 1 & \text{otherwise,} \end{cases}$$

$$V_O(t) := \begin{cases} 0 & \text{if } V_O = 0, \\ V_O - 1 & \text{otherwise.} \end{cases}$$

Finally, let us introduce the following coupling between O_I and O_O.

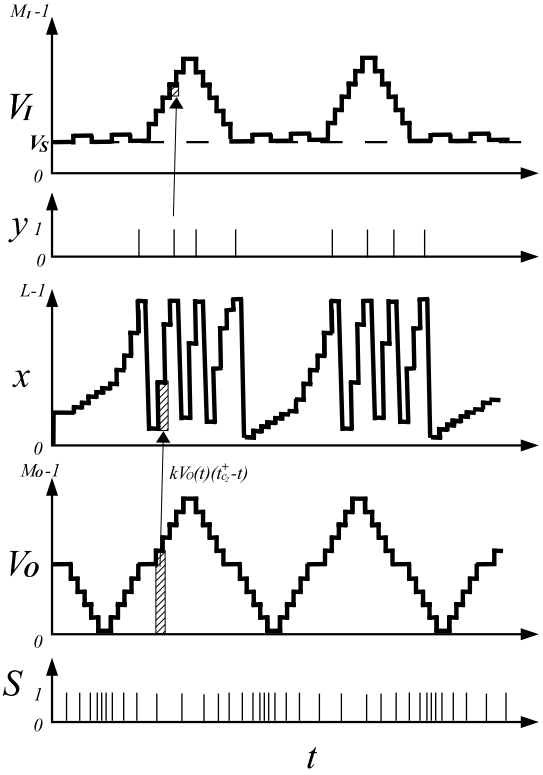

Figure 1: Basic dynamics of the coupled system.

State transition of discrete state for coupling

If $C_O(t) = \uparrow$, then

$$x(t) := \begin{cases} x + kV_O(t) & \text{if } x < L - 1, \\ x + kV_O(t) - (L - 1) & \text{if } x \geq L - 1. \end{cases}$$

Coupling via spike-train $y(t)$

$$y(t) = \begin{cases} 0 & \text{if } x < L - 1, \\ 1 & \text{if } x \geq L - 1, \end{cases}$$

If $y(t) = \uparrow$, then

$$V_I(t) := \begin{cases} V_S & \text{if } V_0 = V_S, \\ V_I - 1 & \text{otherwise.} \end{cases}$$

Fig. 1 shows basic dynamics of the coupled system.

3. Nonlinear filter characteristics and Discussion

Let the spike density of the stimulation spike-train $S(t)$ be sinusoidally modulated as follows.

The instantaneous spike density of $S(t)$ is
$\sigma(1 + \sin(2\pi f_S t))$,

where f_S is referred to as a *modulation frequency* and σ is referred to as a *stimulation intensity*. Fig. 2 shows some

typical simulation results. In order to characterize the response of the coupled system to the stimulation spike-train $S(t)$, let us introduce the following RMS of $V_I - V_S$ for a given stimulation intensity σ.

$$RMS(\sigma) = \sqrt{\frac{1}{T}\int_0^T (V_I - V_S)^2 dt}$$

where T is sufficiently large. In addition, we introduce the following threshold for the RMS.

$$RMS_T > 0 \text{ is a threshold for the } RMS(\sigma).$$

Then we introduce the following *minimum stimulation intensity* Δs to realize $RMS(\sigma) \geq RMS_T$.

$$\Delta s = \min_{\sigma}\{RMS(\sigma) \geq RMS_T\}.$$

Fig. 3 shows characteristics of the minimum stimulation intensity Δs. Note that such a characteristics curve of Δs is often called a *tuning curve* in the literature of cochlea [7],[8]. It can be seen in Fig. 3 that the coupled system realizes nonlinear band-pass filter characteristics. It should be emphasized that these nonlinear band-pass filter characteristics are similar to that of the basilar membrane in a mammalian cochlea [7],[8]. It should be also emphasized that the coupled system mimics not only the nonlinear band-pass filter characteristics of the basilar membrane but also half-wave rectifier characteristics of the inner hair cell in a mammalian cochlea [6]. Hence the coupled system will be useful as a building block of a future cochlea implant that can mimic nonlinear responses of the cochlea.

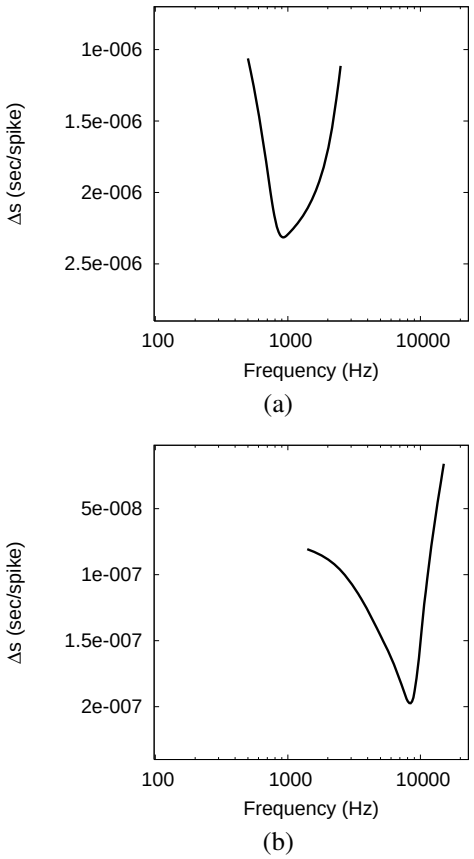

Figure 3: Characteristics of the minimum stimulation intensity Δs. $M_I = N_I = 256$, $M_O = N_O = 128$, $L = 256$, $V_S = 120$. (a) $RMS_T = 26$, $k = 1.1 \times 10^6$, $f_I = 2.0 \times 10^6$, $f_O = 1.8 \times 10^6$. (b) $RMS_T = 44$, $k = 15.2 \times 10^6$, $f_I = 0.2 \times 10^6$, $f_O = 0.16 \times 10^6$

4. Conclusions

In this paper, the coupled system of two asynchronous cellular automaton oscillators was introduced. It was shown that the coupled system can mimic the nonlinear band-pass filter characteristics of the basilar membrane as well as the half-wave rectifier characteristics of the inner hair cell. This work was supported by KAKENHI Grant Number 20318603.

References

[1] T. Matsubara and H. Torikai, Asynchronous Cellular Automaton Based Neuron: Theoretical Analysis and On-FPGA Learning, IEEE Trans. NNLS, Vol. 24, No. 5, pp. 736-748, 2013.

[2] T. Noguchi and H. Torikai, Ghost Stochastic Resonance from Asynchronous Cellular Automaton Neuron Model, IEEE Trans. CAS-II, Vol. 60, No. 2, pp. 111 - 115, 2013.

[3] T. Matsubara, H. Torikai and T. Hishiki, A Generalized Rotate-and-Fire Digital Spiking Neuron Model and its On-FPGA Learning, IEEE Trans. CAS-II, Vol. 58, No. 10, pp. 677-681, 2011.

[4] T. Hishiki and H. Torikai, A Novel Rotate-and-Fire Digital Spiking Neuron and its Neuron-like Bifurcations and Responses, IEEE Trans. NN, Vol. 22, No. 5, pp. 752-767, 2011.

[5] S. Hashimoto and H. Torikai, A novel hybrid spiking neuron: Bifurcations, Responses, and On-chip learning, IEEE Trans. CAS-I, Vol.57, No.8, pp.2168-2181, 2010.

[6] H. Ishimoto and H. Torikai, Asynchronous Cellular Automata Based Hair Cell Models and their Fundamental Characteristics, IEICE Tech. Rep., NLP2012-117, 2013 (in Japanese).

[7] C. Daniel Greisler, From sound to synapse, Oxford University Press, 1998.

[8] J. O. Pickles, An Introduction to the Physiology of Hearing, Emerald Group Publishing Limited, 4th edition, 2012.

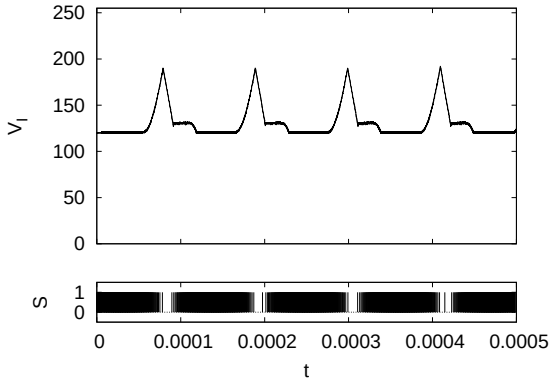

(a) Time-waveforms of O_I. $k = 0$.

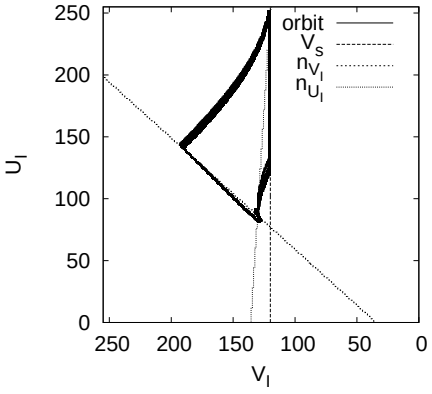

(b) Phase plane of O_I. $k = 0$.

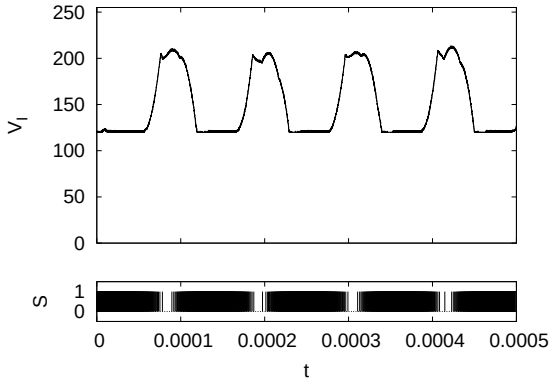

(c) Time-waveforms of O_I. $k = 1.5 \times 10^7$.

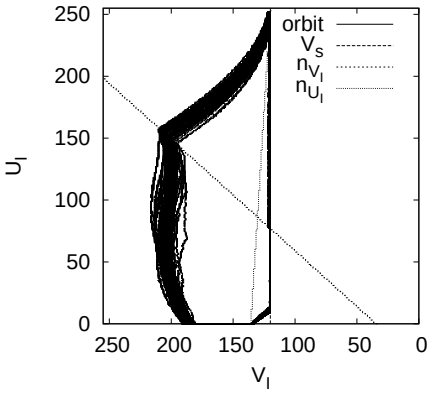

(d) Phase plane of O_I. $k = 1.5 \times 10^7$.

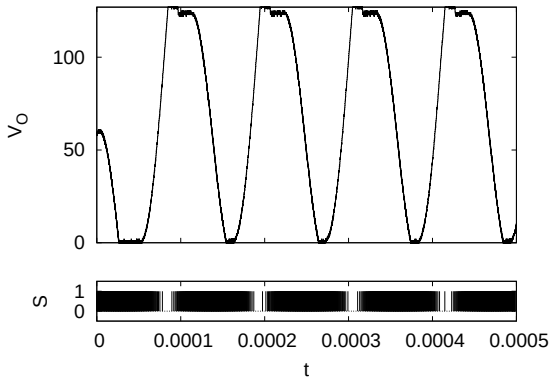

(e) Time-waveforms of O_O.

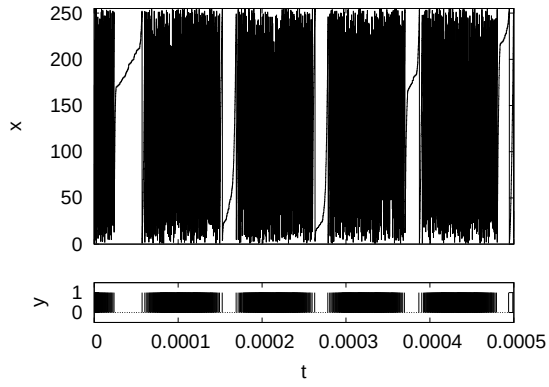

(f) Coupling via discrete state x and spike-train y.

Figure 2: Simulation results. The parameters are $M_I = N_I = 256$, $M_O = N_O = 128$, $L = 256$, $V_S = 120$, and $(n_1, n_2, \cdots, n_8) = (-0.5, 0.78, 16, -7.45, -0.5, 0.4, 16, 0)$. The periods of the clocks $C_I(t)$ and $C_O(t)$ are $f_I = 2.0 \times 10^7$ and $f_O = 1.8 \times 10^7$, respectively. The parameters of the stimulation spike-train $S(t)$ are $f_S = 9.0$kHz and $\sigma = 2.0 \times 10^7$.